Printed
February 3, 1983

RFP-3416
UC-4 CHEMISTRY
DOE/TIC 4500 (Rev. 69)



# THE REACTION OF PLUTONIUM WITH WATER: KINETIC AND EQUILIBRIUM BEHAVIOR OF BINARY AND TERNARY PHASES IN THE Pu+O+H SYSTEM

*John M. Haschke*
*Angelo E. Hodges, III*
*George E. Bixby*
*Robert L. Lucas*

*G. A. Riordan,* Editor
*G. Shekell,* Compositor

**SUBJECT DESCRIPTORS**

**Plutonium Corrosion**
**Plutonium Oxide**
**Plutonium Hydride**
**Phase Equilibrium**
**Hydrolysis**



ROCKWELL INTERNATIONAL
ENERGY SYSTEMS GROUP
ROCKY FLATS PLANT
P.O. BOX 464
GOLDEN, COLORADO 80401

Prepared under Contract DE-AC04-76DP03533
for the
Albuquerque Operations Office
U.S. Department of Energy

## DISCLAIMER

# CONTENTS

## ACKNOWLEDGMENT

The assistance of Dr. R. Chin in collection of XPS data and Mr. J. Fraiser in collection of X-ray diffraction data is gratefully acknowledged.

# THE REACTION OF PLUTONIUM WITH WATER; KINETIC AND EQUILIBRIUM BEHAVIOR OF BINARY AND TERNARY PHASES IN THE Pu+O+H SYSTEM

*John M. Haschke, Angelo E. Hodges, III,*
*George E. Bixby, and Robert L. Lucas*

## ABSTRACT

The kinetic and equilibrium behavior of the Pu+O+H system has been studied by measuring the production of hydrogen gas formed by a sequence of hydrolysis reactions. The kinetic dependence of the $Pu+H_2O$ reaction on salt concentration and temperature has been defined. The metal is quantitatively converted to a fine black powder which has been identified as plutonium monoxide monohydride, PuOH. Other hydrolysis products formed in aqueous media include a second oxide hydride, $Pu_7O_9H_3$, and the oxides $Pu_2O_3$, $Pu_7O_{12}$, $Pu_9O_{16}$, $Pu_{10}O_{18}$, $Pu_{12}O_{22}$, and $PuO_2$. Thermal decomposition products of PuOH include $Pu_2O_2H$ and PuO. A tentative phase diagram for Pu+O+H is presented and structual relationships of the oxide hydrides and oxides are discussed.

## INTRODUCTION

Recent reports from this laboratory have addressed the corrosion of plutonium by water from the domestic supply at Rocky Flats[1] and by synthetic sea water.[2] These studies showed that the corrosion reaction is enhanced by the presence of salt and produces gaseous hydrogen and a fine black powder which was assumed to be a hydroxide of plutonium. Attempts to correlate the data for the mass loss of test samples with the formation of either $Pu(OH)_3$ or $Pu(OH)_4$ plus $H_2$ were unsuccessful. Approximately 0.6 mol of $H_2$ was produced per mol of Pu reacted. For the trihydroxide and tetrahydroxide, the expected molar ratios are 1.5:1 and 2.0:1, respectively. The chemistry of the $Pu+H_2O$ reaction remains undefined.

The present investigation was initiated in an attempt to determine the kinetic dependence of the corrosion rate on salt concentration and to define the chemistry of the corrosion reaction. Although preliminary results showed that samples of plutonium were completely consumed after a few days or weeks in salt water, the production of hydrogen continued. The primary kinetic study has been conducted for more than 450 days and in a stroke of serendipity has provided the key to understanding the complex chemistry of the Pu+O+H system.

## EXPERIMENTAL

Both unalloyed plutonium ($\alpha$-phase, $< 0.2$ at.% impurity) and the $\delta$-stabilized alloy (2.9 at.% Ga) were tested. Inorganic salts were obtained from commercial suppliers.

Kinetic measurements and the preparation of solid hydrolysis products for chemical and X-ray diffraction analysis have been completed in steel (Hastelloy B or 304 stainless) pressure vessels fitted with glass liners. The evacuable test systems have calibrated volumes and include pressure transducers and/or Bourdon gages. The rates and extents of reaction were monitored by PVT methods. Kinetic data for the corrosion of Pu metal by distilled $H_2O$ and by various salt solutions were collected over time periods of several days to several weeks. Tests were conducted at ambient temperature (20-25 °C) and at 100 °C in heated PVT systems. One experiment at ambient temperature has been conducted concurrently with other tests for more than one year. In this test, an 8.400 g sample of unalloyed Pu was submerged in 10 $cm^3$ of 1.0*M* $CaCl_2$ solution contained in a PVT system with a free volume of

94.93 $cm^3$. After 100 days, the $H_2$ pressure reached the 10 atm calibration limit of the transducer. The pressure was reduced to 6.8 psi and maintained in the 6.8-10 psi range until day 269. After that point, the $H_2$ pressure was confined to the 1-2 atm range.

Samples of the black product formed by the initial reaction of Pu with $H_2O$ were prepared in PVT systems. Weighed samples of unalloyed metal were combined with small quantities ($< 1$ $cm^3$) of 0.01*M* NaCl solution and the production of $H_2$ was monitored. After the appropriate quantity of $H_2$ had been produced (in this case, 0.5 mol $H_2$ per mol Pu), the reaction was stopped by removing the water. In some cases the product was dried in the PVT apparatus under dynamic vacuum. In other tests, the sample was dried using synthetic 4A molecular sieve. Samples for microbalance analysis (0.60-0.65 g) were prepared in silica microbalance buckets and transferred directly to the balance for thermogravimetric measurements. Some samples were dried prior to transfer, and others were dried over molecular sieve while their mass losses were measured as a function of time. Thermogravimetric data were obtained in vacuum or hydrogen atmospheres using heating rates of 2-10 °C $min^{-1}$.

The loss of hydrogen by the hydrolysis product was also measured using a dual-chamber PVT apparatus. One chamber was used for sample preparation as described above. The second volume contained molecular sieve and was used to quantify the amount of $H_2$ removed from the system and the amount generated during drying. Attempts were made to quantify the production of $H_2$ during thermal decomposition of the hydrolysis product.

The solid product from the Pu+$H_2O$ reaction was characterized using X-ray diffraction and photoelectron spectroscopy. Diffraction data were obtained with wet and dry samples. Lattice parameters were calculated using data for selected high angle reflections. The XPS data were collected using a metal sample which was coated with an adherent product layer by exposure to 0.01*M* NaCl solution for several hours. Gas samples were analyzed by mass spectrometry.

## RESULTS

### Kinetic Behavior of the Pu+$H_2O$ System

Water corrosion of plutonium is a complex process which produces hydrogen at a measurable rate for more than a year. The time dependence of $H_2$ formation in the extended hydrolysis experiment is shown in Figures 1 and 2. Hydrogen is produced in a sequence of constant-rate steps which have successively lower reaction rates for a given range of $H_2$ overpressure. Mass spectrometric analysis shows that the purity of the product $H_2$ is greater than 99.9 mol percent. Examination of the solid products present in several tests which were interrupted after 0.50 mol of $H_2$ had been produced per mol of Pu showed that the metal samples were completely consumed. This observation demonstrates that reaction of the metal is complete at the first slope change in Figure 1. The product is a fine black precipitate which settles out with a bulk density of approximately 0.8 g Pu·$cm^{-3}$. The bulk density of the dried product is $(2.1 \pm 0.1)$g·$cm^{-3}$.

The corrosion rate of plutonium by water varies both with salt concentration and with the nature of the salt. The rate results from earlier studies with tap water[1] and sea water[2] have been combined with results for distilled water and for $CaCl_2$ solutions of various concentrations in Figure 3. Over the anion concentration range $1 \times 10^{-7} \leq [X] \leq 1.0M$, the corrosion rate R in mgPu·$cm^{-2}$·$hr^{-1}$ is approximated by Equation 1.

$$\log_{10} R = 1.2 + 0.7 \log_{10} [X] \qquad (1)$$

Noticeable deviations from this relationship are observed at salt concentrations greater than 1 molar. As shown by the results in Table 1, the corrosion rate is also altered by changes in the anion and, to a lesser extent, by changes in the cation. These results suggest that Equation 1 applies only to salt solutions which contain predominately chloride. A small change in the behavior of the cations across the first row transition series is seen in Table 1. The maximum corrosion rates are observed near the middle of the d-block series. The effects of salt concentration on the rates of subsequent hydrolysis reactions which do not involve Pu metal are unknown.

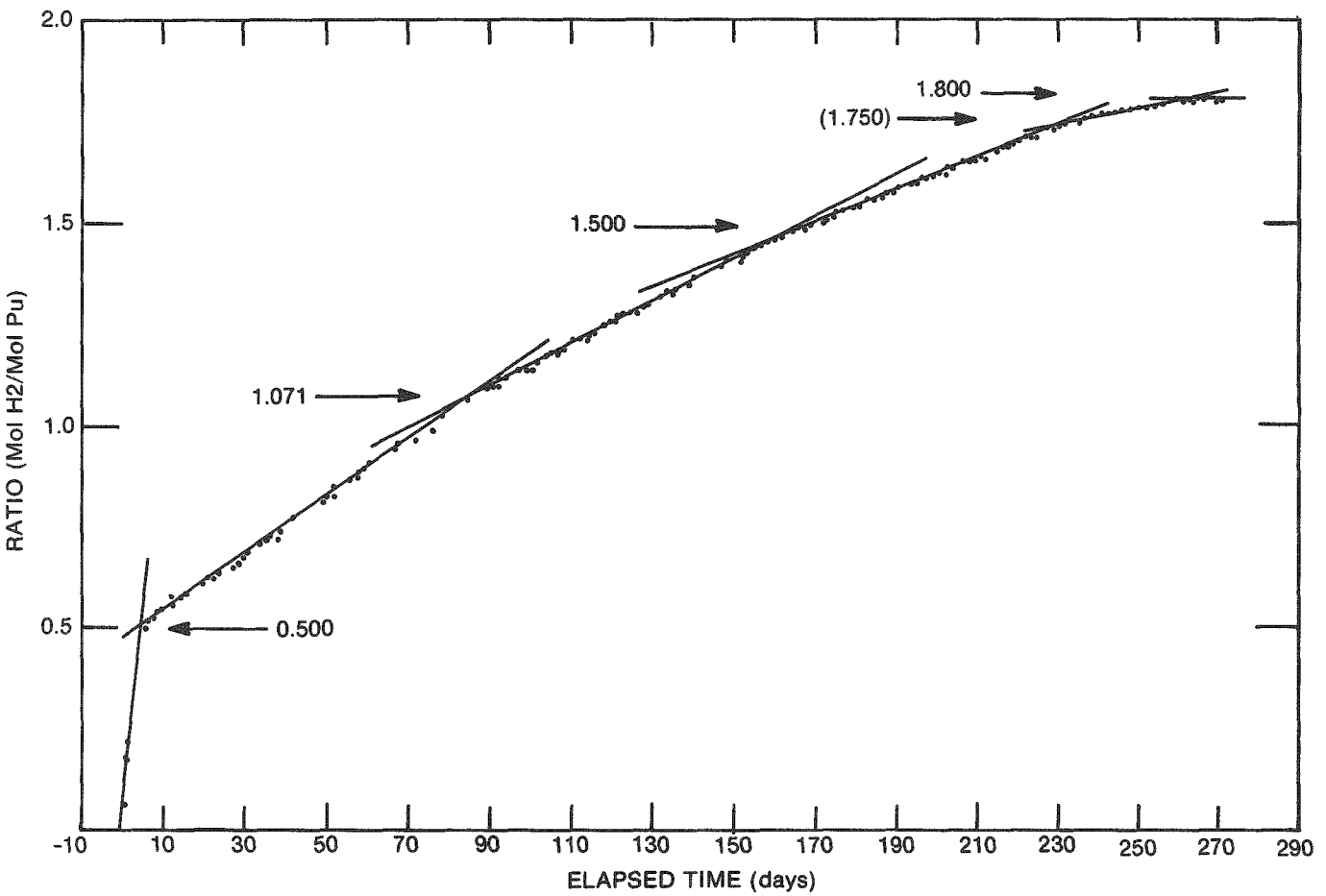


FIGURE 1. The Time Dependence of the $H_2$ :Pu Ratio for the Reaction of 1*M* $CaCl_2$ Solution at 25 °C

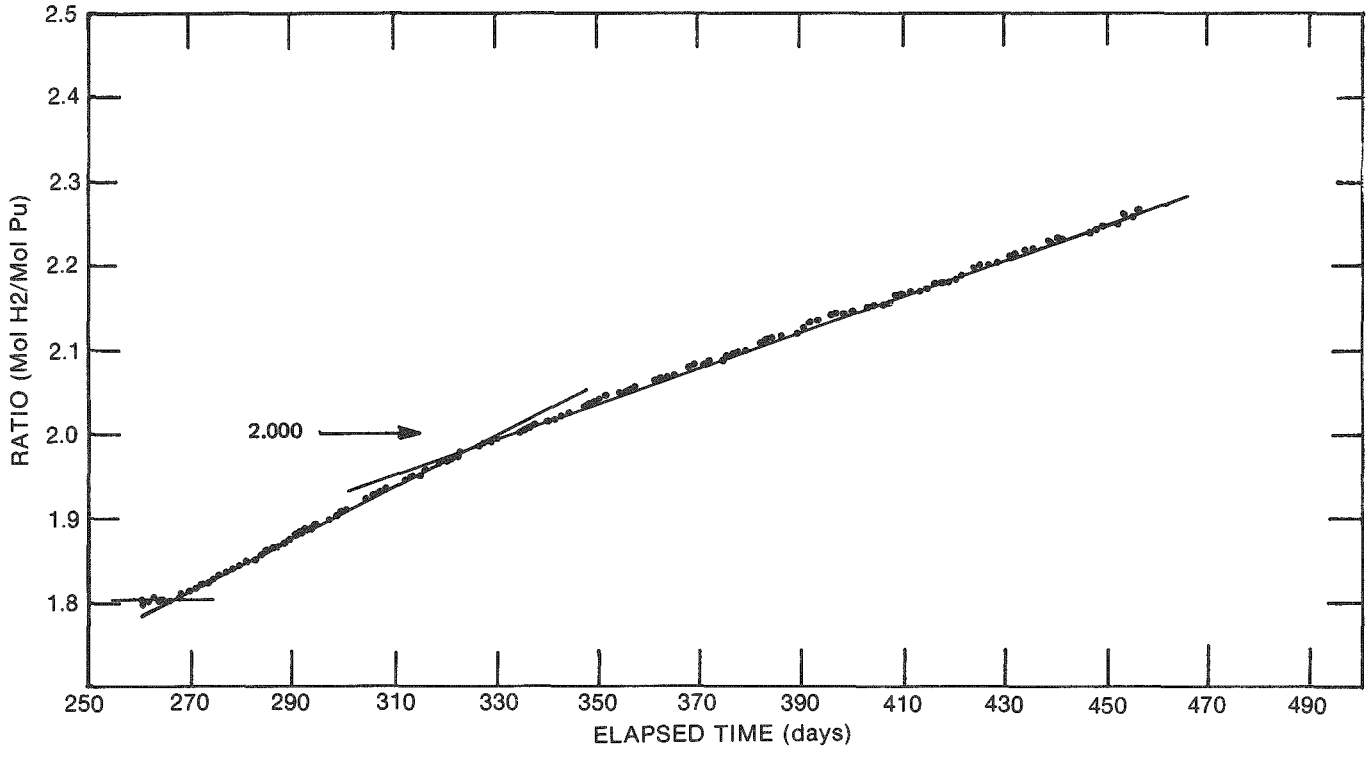


FIGURE 2. The Time Dependence of the $H_2$ :Pu Ratio for the Reaction of 1*M* $CaCl_2$ Solution at 25 °C

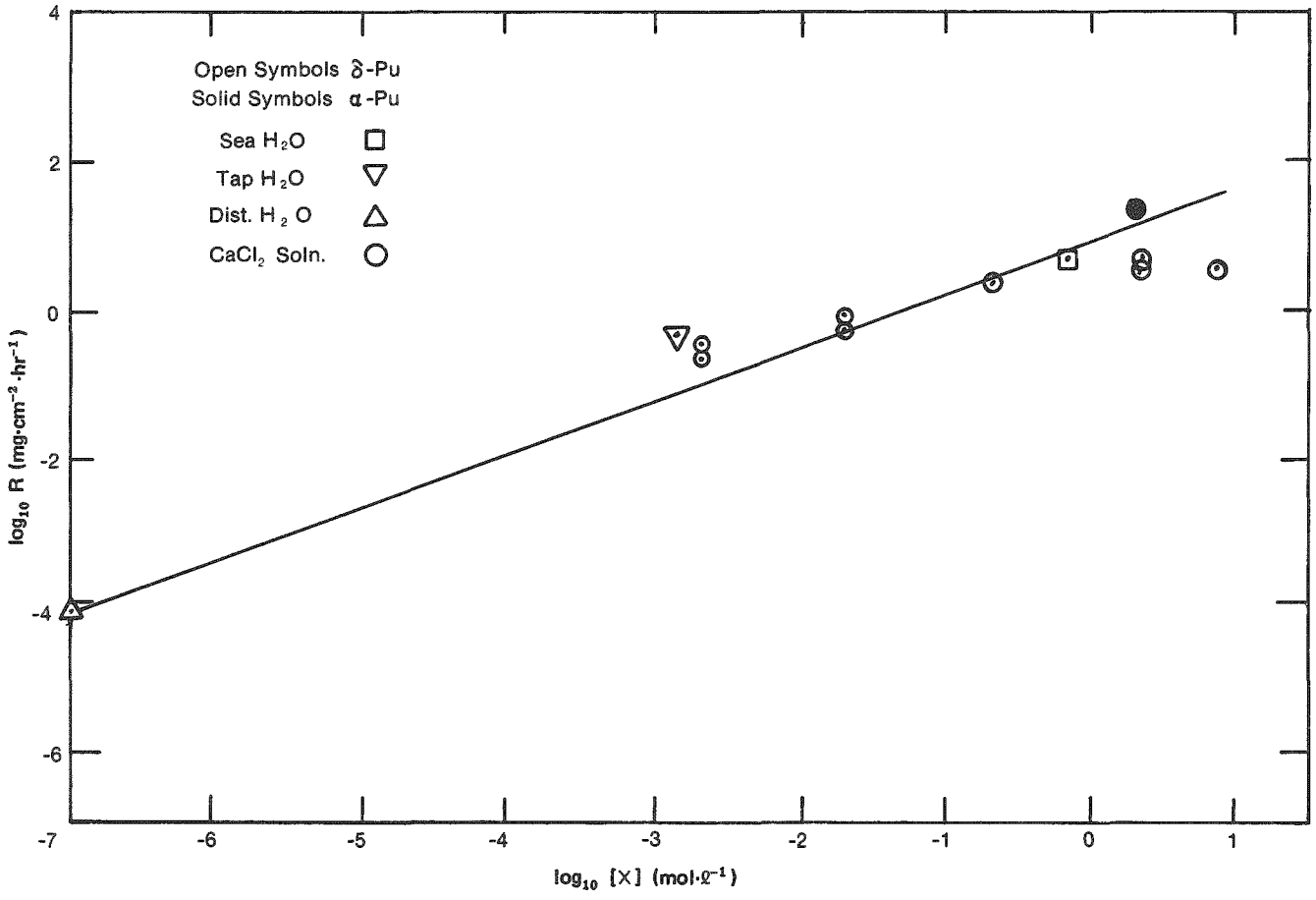


FIGURE 3. The Salt Concentration Dependence of the Rate of the Pu + $H_2O$ Reaction at 25 °C

TABLE 1. Corrosion Rates of α-Phase Pu by 1.0*M* Salt Solutions at 25 °C

| Salt Solution | Corrosion Rate: mmol $H_2 \cdot cm^{-2} \cdot hr^{-1}$ | | Corrosion Rate: mg $Pu \cdot cm^{-2} \cdot hr^{-1}$ * | |
|---|---|---|---|---|
| $CaCl_2$ | 0.065 | | 31 | |
| $FeCl_2$ | 0.38 | ± 0.07 | 182 | ± 33 |
| $CoCl_2$ | 0.33 | | 158 | |
| $NiCl_2$ | 0.39 | ± 0.07 | 186 | ± 33 |
| $CuCl_2$ | 0.19 | | 91 | |
| $FeCl_3$ | 0.32 | | 153 | |
| $Fe(NO_3)_3$ | 0.0050 | | 2.4 | |

*The conversion from mmol $H_2 \cdot cm^{-2} \cdot hr^{-1}$ to mg $Pu \cdot cm^{-2} \cdot hr^{-1}$ are based on the reaction ratio of 0.5 moles $H_2$ per mol of Pu.

TABLE 2. Mass Gain Data for Reaction of Pu* With $H_2O$

| Test No. | Drying Method | Mass Gain (%) |
|---|---|---|
| 1 | Vacuum | 6.75 |
| 2 | Vacuum | 6.79 |
| 5 | 4A Sieve | 7.14 |

*Metal samples were in the range 0.64 to 0.65 grams.

The temperature dependence of the $Pu+H_2O$ reaction kinetics has been obtained from results with 1*M* $NiCl_2$ solution. Arrhenius analysis of the measured rate at 100 °C (2.3 ± 0.1 mmol $H_2 \cdot cm^{-2} \cdot hr^{-1}$) and the value for 25 °C from Table 1 yield the relationship for the rate in mmol $H_2 \cdot cm^{-2} \cdot hr^{-1}$.

$$\ell nR = 7.78 - (2.59 \times 10^3)/T \qquad (2)$$

The activation energy derived for the corrosion process from Equation 2 is 5.2 kcal·mol$^{-1}$. It should be noted that different kinetics are observed at 100 °C if the metal and solid product do not remain submerged in the liquid phase. The generation of $H_2$ is rapid (~16 mmol $H_2 \cdot cm^{-2} \cdot hr^{-1}$) and indicates that the plutonium is completely converted to the tetravalent state.

The corrosion rate is also enhanced by a decrease in the hydrogen overpressure, but the magnitude of the effect is not well defined. The observed change is seen by comparing the rates of $H_2$ production in Figures 1 and 2. After reduction of the pressure from 8.3 atm at day 269, the rate increased by at least a factor of 2.5 or more.

## Chemistry of the $Pu+H_2O$ System

Identification of the solid hydrolysis product formed by the $Pu + H_2O$ reaction is essential for interpreting the chemistry of the continuing reaction seen in Figures 1 and 2. The formation of 0.5 mol $H_2$ per mol of Pu in the first step in Figure 1 is consistent with the processes described by Equations 3 and 4.

$$Pu(s) + 2H_2O(\ell) \rightarrow Pu(OH)_2H(s) + \tfrac{1}{2}H_2(g) \qquad (3)$$

$$Pu(s) + H_2O(\ell) \rightarrow PuOH(s) + \tfrac{1}{2}H_2(g) \qquad (4)$$

Since the second slope change at $H_2$ :Pu = 1.07 is consistent with the hydrolysis of $Pu(OH)_2H$ to form 1/7 $Pu_7(OH)_{18}H_3$ plus 4/7 mol of $H_2$, and since $M(OH)_2X$ and $M_7(OH)_{18}X_3$ (X = Cl, Br, I, $NO_3$) are stable phases in the lanthanide + hydroxide + monovalent anion systems,[3] Equation 3 was initially given preference. However, experimental results from a number of techniques demonstrate that the solid product is not hydroxide or hydrated oxide. Since the product forms with distilled water and since chloride analyses of the solid product show chloride contents below detectable limits, the possible formation of oxide chlorides or hydroxide chlorides can be excluded. The initial hydrolysis product is a fine coal-black powder which seems to exhibit a slight greenish hue after drying. Dried samples have been transported and stirred in air without evidence of reaction. The product has been identified as plutonium monoxide monohydride, PuOH.

Important evidence for the form of PuOH is provided by the mass gain data presented in Table 2. The results of vacuum drying and drying with molecular sieve are in good agreement. In both cases, the hydrolysis reaction of a weighed metal sample was stopped at $H_2$ :Pu = 0.5. The average mass gain of 6.89 ± 0.21% is in good agreement with the theoretical value of 7.11% for formation of PuOH according to Equation 4. The theoretical change for Equation 3 is 14.64 percent. However, the formation of $Pu(OH)_2H$ (i.e., $PuOH \cdot H_2O$) cannot be excluded since dehydration of the

TABLE 3. X-Ray Diffraction Intensities for PuOH and Literature Values for $PuO_2$*

| hkℓ | I/Io (%) PuOH | $PuO_2$ |
|---|---|---|
| 111 | 100 | 100 |
| 200 | 34 | 20 |
| 220 | 45 | 80 |
| 311 | 42 | 80 |
| 222 | 8 | 20 |
| 400 | 5 | - |
| 331 | 11 | 50 |
| 420 | 10 | 50 |
| 422 | 8 | 50 |
| 333 | 9 | 50 |

*ASTM Powder File 6-360

hydroxide hydride could occur during drying. To investigate this possibility, samples of the wet product were dried on the microbalance at 25 °C with a charge of molecular sieve in the hangdown tube. If $PuOH \cdot H_2O$ were stable, a slope change should be observed at the theoretical hydrate composition in the drying curve. In all cases, the curves were smooth and showed no evidence for the existence of hydrates.

The X-ray diffraction results for the first hydrolysis product are consistent with the formation of the monoxide monohydride. Data for both the vacuum dried and the wet samples show only a face centered cubic (Fm3m) phase; the derived lattice parameters are (5.400 ± 0.007) and (5.401 ± 0.002) Å, respectively. Since the lattice parameters of $PuH_2$ and $PuO_2$ are 5.359 and 5.397 Å, respectively,[4] the presence of an equimolar mixture of dioxide and dihydride or a mixture of dioxide and an amorphous phase cannot be excluded. However, it seems rather unlikely that precisely half of the hydrogen reacts with Pu to form $PuH_2$ while the other half is released as $H_2$. The formation of a single stoichiometric product is most probable. The relative intensities of the low angle reflections are presented in Table 3. A noticeable broadening of the lines and the absence of back reflections indicate that the products are only moderately crystalline. An average particle size of 66 Å is derived from the X-ray data.

Results of thermogravimetric analysis show that the hydrolysis product is PuOH. The decomposition curve for a dried product is presented in Figure 4. The sample was first dried to constant mass at 25 °C with molecular sieve. An additional mass loss was observed when the balance chamber was evacuated and during slow heating of the sample to 80 °C. The 1.5 mg loss is attributed to desorption of residual moisture. Between 80 and 100 °C, the mass was constant. When the sample was heated in dynamic vacuum ($1 \times 10^{-7}$ torr ultimate vacuum) at a constant rate of 2.2 $°C \cdot min^{-1}$, the curve in Figure 4 was obtained. Decomposition of PuOH begins at approximately 105 °C and is complete at approximately 195 °C. The observed changes in the mass loss rate were tracked by pressure changes in the vacuum chamber. A noticeable slope change at 0.2 % loss is consistent with the formation of a second oxide hydride, $Pu_2O_2H$ (0.196 % theoretical loss). The total mass loss of $H_2$ is in excellent agreement with the theoretical value of 0.391 % shown by the horizontal arrow. Whether the decomposition residue is a mixture of plutonium dioxide and metal or whether it is the monoxide, PuO, cannot be established from these data. The mass changes observed on heating the residues from several tests in air or oxygen to 500 °C are in good

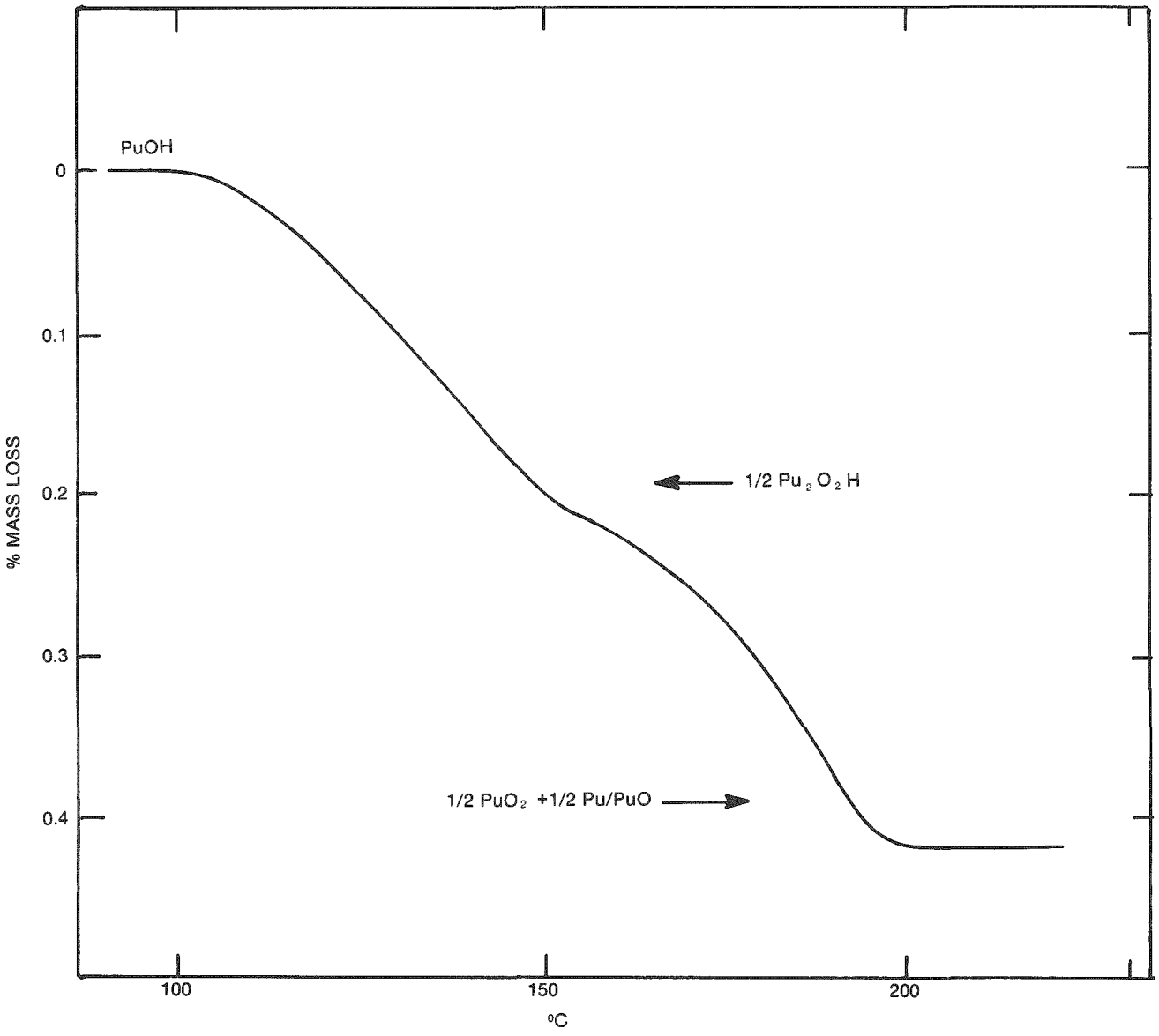


FIGURE 4. Thermogravimetric Results for Decomposition of PuOH in Dynamic Vacuum at a Heating Rate of 2.2 $^{\circ}C \cdot min^{-1}$

agreement with the theoretical value for conversion of the sample to $PuO_2$.

Experiments to monitor the decomposition of the hydrolysis product by PVT methods show that gaseous $H_2$ is formed in the temperature range indicated by the thermogravimetric data. Quantitative removal of $H_2$ from the reaction chamber shows that the solid product does not lose detectable amounts of $H_2$ during venting of the product overpressure or during drying with molecular sieve. Attempts to quantify the $H_2$ release during thermal decomposition have been unsuccessful because of reaction between the solid residue and hydrogen. This behavior will be addressed in the discussion of the decomposition product.

The X-ray photoelectron spectroscopic data for the hydrolysis and decomposition products provide additional insight into their identities. The oxygen O(1s) and Pu(4f 7/2) spectra for the initial and final products are shown in Figures 5 and 6, respectively. The O(1s) spectrum of the hydrolysis product in Figure 5 is bifurcated. The high energy peak is in good agreement with the binding energy of oxygen

FIGURE 5. Comparison of the XPS O(1s) Spectrum of the Initial Product of the Pu + $H_2O$ Reaction With That of Its Decomposition Residue

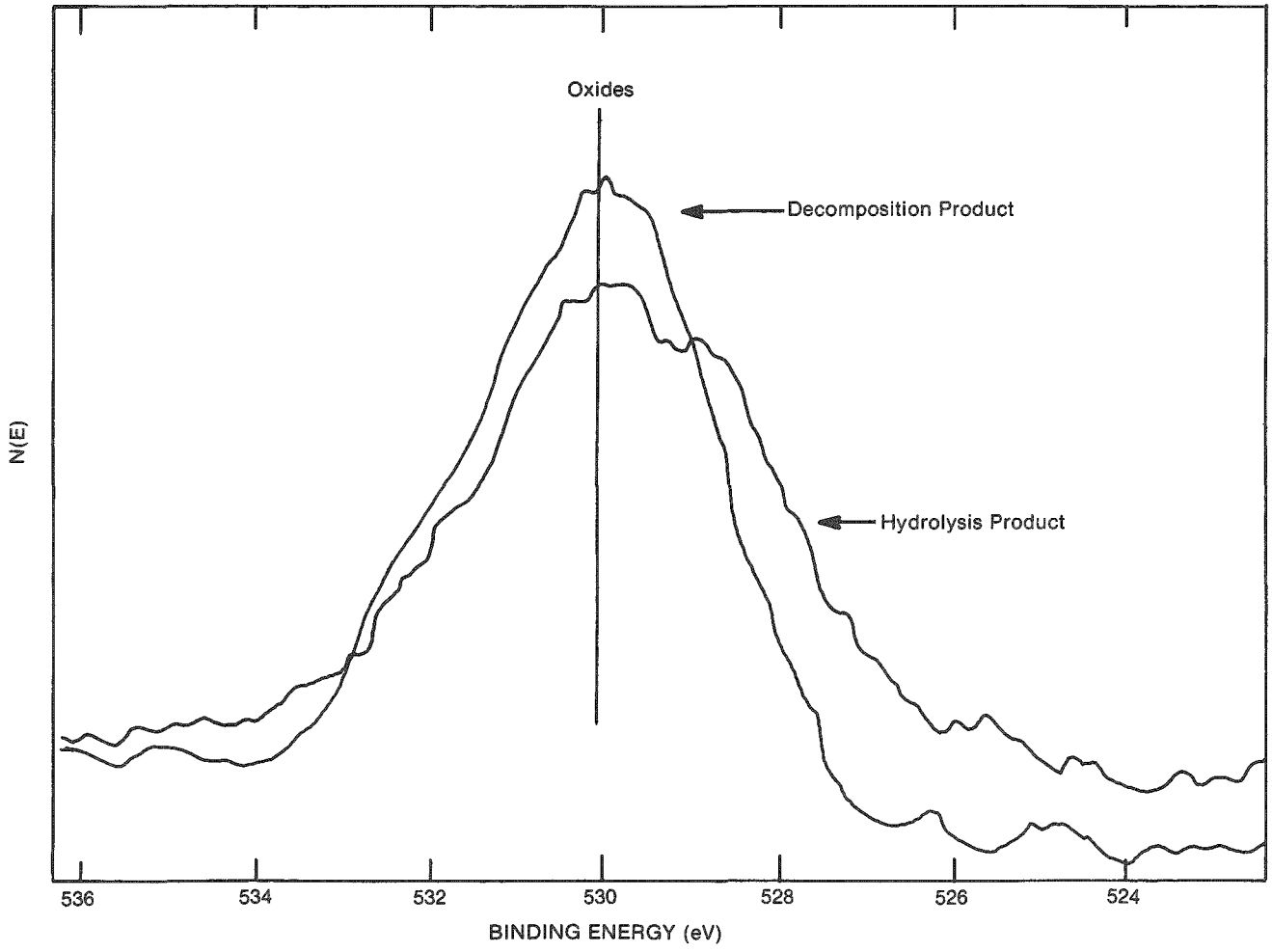

in the plutonium oxides (530.1 eV) (see Reference 5) and suggests that the sample surface was contaminated with plutonium oxide. The low binding energy branch is consistent with the presence of an electron donating species such as hydride in the lattice. After the heating step in which the evolution of $H_2$ was verified by residual gas analysis, the O(1s) peak shows that only plutonium oxides are present. The corresponding Pu(4f 7/2) spectra suggest that neither the hydrolysis nor decomposition products is a known oxide of plutonium. Although a slight high energy broadening again indicates the presence of $PuO_2$ in both products, the maxima lie between the binding energies of $PuO_2$ (426.1 eV) and $Pu_2O_3$ (424.4 eV). Evidence for metallic plutonium is not found in either spectrum. The important results are that oxygen in the hydrolysis product exists in a reducing environment, that an oxide other than $PuO_2$ or $Pu_2O_3$ is formed during thermal decomposition, and that plutonium metal does not form during decomposition.

Identification of the initial hydrolysis product as the monoxide monohydride virtually precludes occurrence of hydroxide-containing solid products in the sequence of hydrolysis reactions which produce hydrogen for more than a year. The presence

FIGURE 6. Comparison of the XPS Pu(4f 7/2) Spectrum of the Initial Product of the Pu + $H_2O$ Reaction With That of Its Decomposition Residue

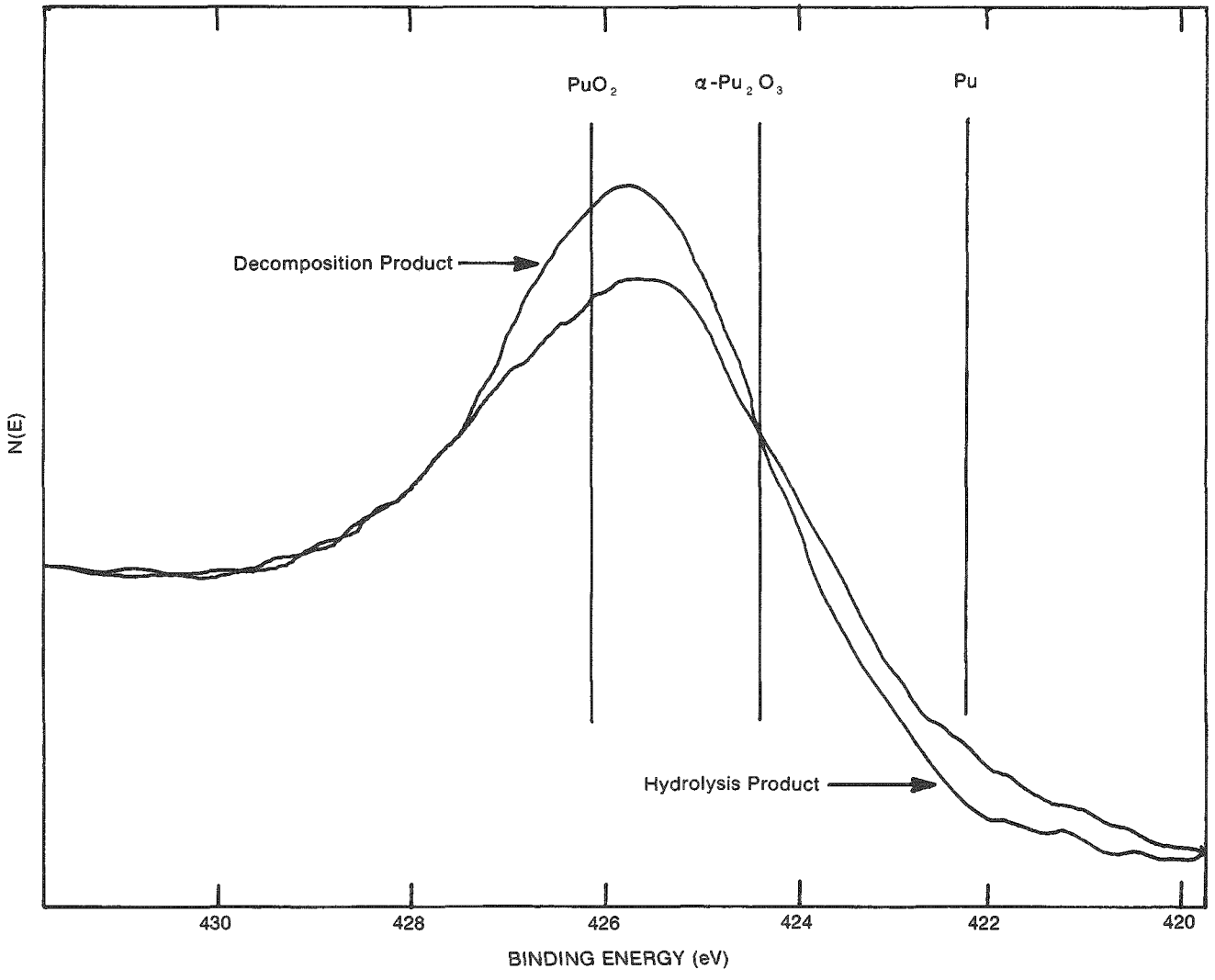

of linear regions and sharp slope changes in Figures 1 and 2 implies that successive equilibrium reactions occur in the system. Assignment of each linear region to a specific hydrolysis reaction is predicated on the existence of successive reactions in which one solid phase reacts with water to produce a second solid and hydrogen. Since hydrolysis of the second phase cannot start until the first solid is completely consumed, the amount of $H_2$ produced during a given linear segment defines the stoichiometry of the reaction. A check of this approach is provided by the fact that all proposed reactions must be consistent with existing knowledge of plutonium chemistry.

A more careful examination of the rate data in Figures 1 and 2 is necessary before an attempt can be made to formulate the hydrolysis reactions. The regions around the $H_2$ :Pu ratio of 1.75 in Figure 1 and the initial portion of Figure 2 are expanded in Figures 7 and 8, respectively. In addition to the slope changes near $H_2$ :Pu = 0.50 and 1.07 in Figure 1, breaks are also observed at 1.71, 1.78, and 1.80. In addition to the break at 2.00, Figure 8 shows that a change also occurs at 1.83. The results of linear regression analysis of the constant slope regions and their mathematically determined $H_2$ :Pu intersection points are given in Table 4. The sequence of reactions which describe the hydrolysis processes and account for the intersection points in Table 4 are given in Table 5. The theoretical $H_2$ :Pu ratios shown by the horizontal arrows in Figures 1, 2, 7, and 8 are in remarkable agreement with the data.

FIGURE 7. The Time Dependence of the $H_2$ :Pu Ratio for the Reaction of 1*M* $CaCl_2$ at 25 °C

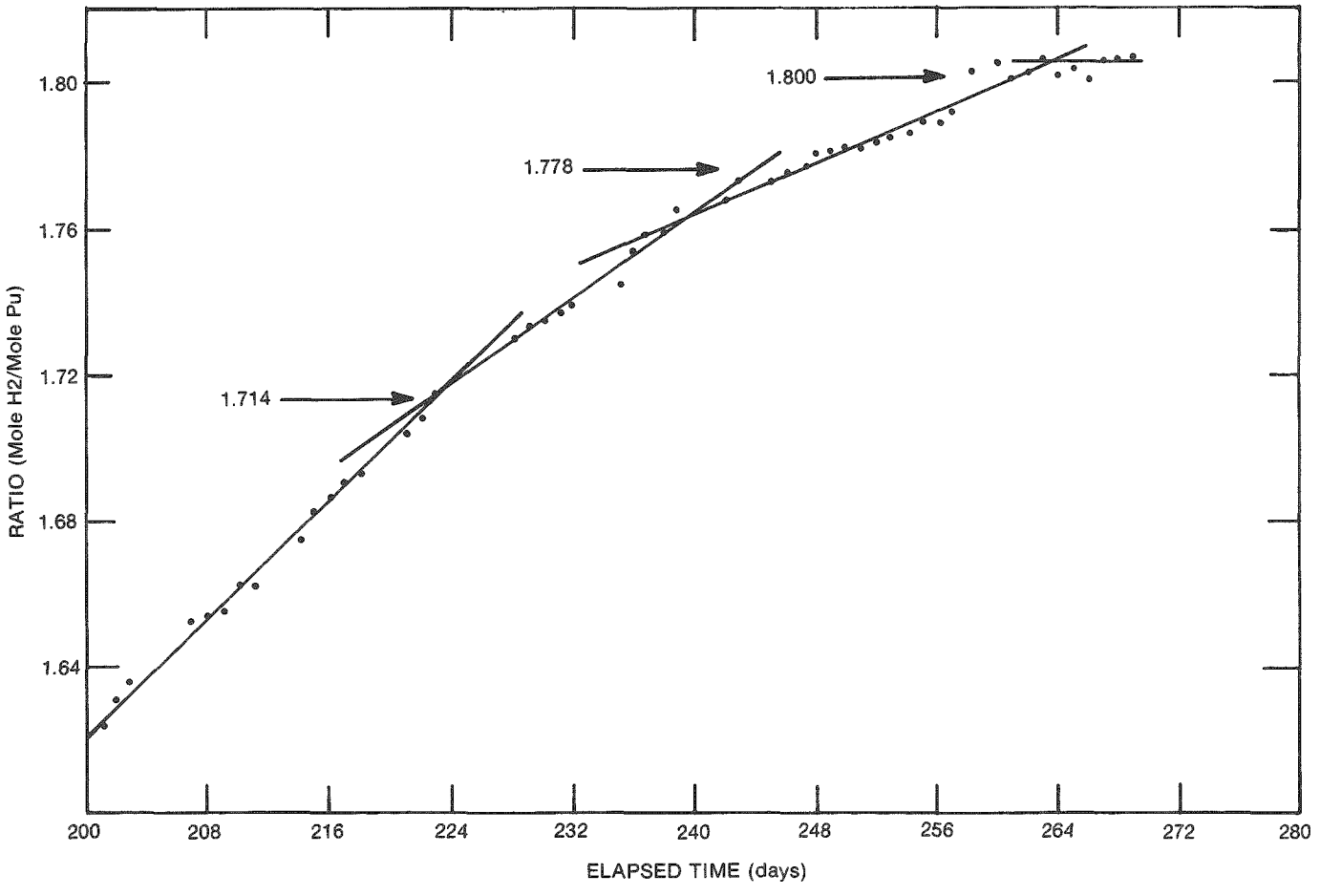

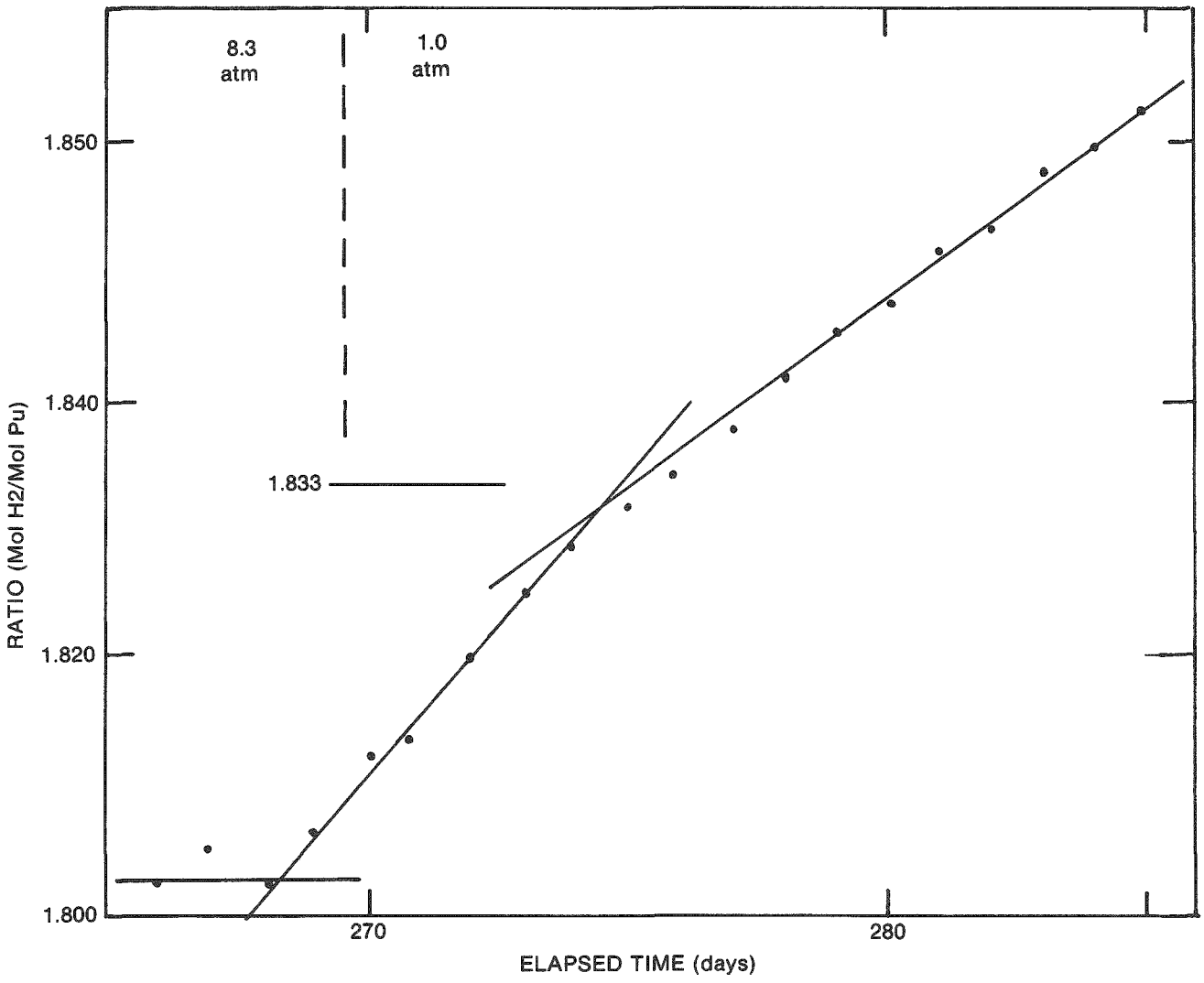


FIGURE 8. The Time Dependence of the $H_2$ :Pu Ratio for the Reaction of 1*M* $CaCl_2$ Solution at 25 °C

TABLE 4. Linear Regression Results and Intersection Points for Segments of Kinetic Data in the Form mol $H_2$·mol $Pu^{-1}$ = A + (B × $10^{-3}$)t

| Time Range (days) | A (mol $H_2$·mol $Pu^{-1}$) | B (mol $H_2$·mol $Pu^{-1}$·$da^{-1}$) | r | Intersection Point (mol $H_2$·mol $Pu^{-1}$) |
|---|---|---|---|---|
| 0-5 | (0.04834 ± 0.0274 ) | (92.672 ± 11.640 ) | 0.977 | (0.507 ± 0.006) |
| 6-87 | (0.47236 ± 0.00206) | ( 7.0064 ± 0.0465) | 0.999 | (1.078 ± 0.023) |
| 88-167 | (0.62826 ± 0.00415) | ( 5.2026 ± 0.0320) | 0.999 | (1.455 ± 0.038) |
| 168-223 | (0.81236 ± 0.00523) | ( 4.0387 ± 0.0267) | 0.999 | (1.716 ± 0.170) |
| 224-243 | (1.06157 ± 0.03372) | ( 2.9281 ± 0.1435) | 0.988 | (1.763 ± 0.118) |
| 244-263 | (1.33778 ± 0.02612) | ( 1.7751 ± 0.1031) | 0.972 | (1.803 ± 0.002) |
| 264-269* | (1.80280 ± 0.00262) | 0 | -- | -- |
| 270-274 | (0.62591 ± 0.09471) | ( 4.3902 ± 0.3901) | 0.968 | (1.831 ± 0.181) |
| 275-327 | (0.99684 ± 0.00389) | ( 3.0386 ± 0.0013) | 0.999 | (1.993 ± 0.016) |
| 328-450 | (1.29948 ± 0.00307) | ( 2.1154 ± 0.0078) | 0.999 | -- |

*Regression analysis of these data shows a positive slope; however, the value (0.56 × $10^{-3}$ mol $H_2$·mol $Pu^{-1}$·$da^{-1}$) and the correlation coefficient (0.53) are both low, and the data have been averaged. It is not known whether the 8.3 atm $H_2$ pressure is the equilibrium pressure for the $Pu_{10}O_{18}$ + $Pu_{12}O_{22}$ region or whether the reaction rate is finite, but less than the scatter in the data.

TABLE 5. Sequence of Hydrolysis Reactions in the Pu+O+H System at 25 °C

| Reaction | Theoretical mol$H_2$ :molPu |
|---|---|
| $Pu + H_2O \rightarrow PuOH + \frac{1}{2}H_2$ | 0.500 |
| $PuOH + 2/7\ H_2O \rightarrow 1/7\ Pu_7O_9H_3 + 4/7\ H_2$ | 1.071 |
| $1/7\ Pu_7O_9H_3 + 3/14\ H_2O \rightarrow \frac{1}{2}\ Pu_2O_3 + 3/7\ H_2$ | 1.500 |
| $\frac{1}{2}\ Pu_2O_3 + 3/14\ H_2O \rightarrow 1/7\ Pu_7O_{12} + 3/14\ H_2$ | 1.714 |
| $1/7\ Pu_7O_{12} + 4/63\ H_2O \rightarrow 1/9\ Pu_9O_{16} + 4/63\ H_2$ | 1.778 |
| $1/9\ Pu_9O_{16} + 1/45\ H_2O \rightarrow 1/10\ Pu_{10}O_{18} + 1/45\ H_2$ | 1.800 |
| $1/10\ Pu_{10}O_{18} + 1/30\ H_2O \rightarrow 1/12\ Pu_{12}O_{22} + 1/30\ H_2$ | 1.833 |
| $1/12\ Pu_{12}O_{22} + 1/6\ H_2O \rightarrow PuO_2 + 1/6\ H_2$ | 2.000 |

A final, but particularly interesting material encountered in the course of this study is the product formed by thermal decomposition of plutonium monoxide monohydride. In marked contrast to the coal-black color of PuOH, the product has a steel-grey color and a metallic luster. As noted above, the identity of the product cannot be established from the mass-loss data in Figure 4, but the chemical behavior of the product indicates that it is plutonium monoxide, PuO. In the course of one thermogravimetric analysis similar to that shown in Figure 4, heating of the sample was continued to 500 °C. In the temperature interval between 190 and 435 °C, the sample mass was constant; no reaction occurred between the sample and the residual gases (1 × $10^{-4}$ torr) in the microbalance system. At Temperatures greater than 435 °C, the sample became reactive and gained mass at a constant rate. Even after the sample had been cooled rapidly to 25 °C it continued to gain

mass at the same rate. This behavior suggests that the product was somehow altered by heating above 435 °C.

The results of further microbalance tests with the product obtained in the thermogravimetric study described by Figure 4 are particularly interesting. Since formation of an equimolar $PuO_2$ + $PuH_2$ mixture during the initial hydrolysis step could not be excluded by other results, a test was designed to help resolve this question. The temperature range of $H_2$ loss by the product is approximately 200 °C lower than that observed for $PuH_2$ (see Reference 6), but such a difference might result from a high surface area of the hydride formed by water. Since the decomposition residue was assumed to be a mixture of $PuO_2$ and Pu, the behavior of the hydride with a similar particle size could be determined by exposing the residue to $H_2$, forming a known mixture of oxide and hydride, and comparing its decomposition behavior with those of the hydrolysis product and of bulk $PuH_2$. After the residue (see Figure 4) had been cooled to room temperature, 100 torr of high purity $H_2$ from a $UH_3$ reaction bed was introduced, but no reaction occurred. The sample was then heated to 100 °C under that $H_2$ pressure. When no reaction could be detected after 0.5 hr, it was assumed that somehow an error had been made and the sample had been inadvertently oxidized to $PuO_2$. To verify that conclusion, the balance chamber was evacuated and $O_2$ gas was introduced at 100 °C. The ensuing reaction was so rapid and exothermic that the silica bucket melted and fell from the balance.

Thermal decomposition of the initial hydrolysis product in a $H_2$ atmosphere has also helped to identify the decomposition product. This test also addresses the question of a possible $PuO_2$ + $PuH_2$ mixture because the equilibrium behavior of hydride must be independent of particle size. If hydride is heated under a constant $H_2$ pressure, its composition will follow that described by a known temperature-composition isobar.[7] The thermogravimetric curve for 200 torr $H_2$ is shown in Figure 9. The decomposition is similar to that observed in vacuum and demonstrates that the hydrolysis product is not a mixture containing hydride. However, the reaction of the residue with $H_2$ at 215-220 °C was not anticipated. The mass gain is accompanied by an exotherm in the heating curve and is in good agreement with the formation of a 2:1 mixture of $Pu_2O_3$ and $PuH_{2.4}$. The equilibrium hydride composition at 200 °C and 200 torr $H_2$ pressure is $PuH_{2.5}$.[7] When the product was heated in vacuum, its decomposition kinetics verified the presence of plutonium hydride.[6]

The microbalance data indicate that the decomposition product is plutonium monoxide. Thermal decomposition of PuOH apparently provides a low temperature route for its preparation. The onset of reaction with low pressure gases at 435 °C is attributed to the disproportionation of PuO into a reactive mixture of $Pu_2O_3$ and Pu. This behavior is consistent with the expected metastability of the phase.[5] The monoxide reacts at lower temperatures with higher pressures of $O_2$ or $H_2$ to form $PuO_2$ or a $Pu_2O_3$ + $PuH_X$ mixture, respectively.

## CONCLUSIONS

### Kinetics of the Hydrolysis Reactions

The kinetic behavior of various salt solutions in Figure 3 support a prior suggestion that aqueous corrosion of plutonium is catalyzed by salt.[2] It is not surprising that variations in catalytic effect are seen with different anions and to a lesser extent with different cations. The ions are probably involved in the transfer of electrons from Pu to $H_2O$. Of greatest interest is the rapid corrosion rates in common salt solutions such as sea water. Earlier reports describe the reaction of water with plutonium as "very slow at room temperature."[8] If submerged in sea water at 25 °C a 1-mm thick sheet of metal will be converted to PuOH powder in approximately 16 days. The literature description of corrosion rates is seriously in error if typical amounts of salt are present. Our data also indicate that the reaction kinetics of gaseous and liquid water are different and predictions about the behavior of the vapor phase should not be made on the basis of these results.

As noted previously, the reactions of $H_2O$ with plutonium and with the successive solid products are equilibrium processes. Precise linear regions

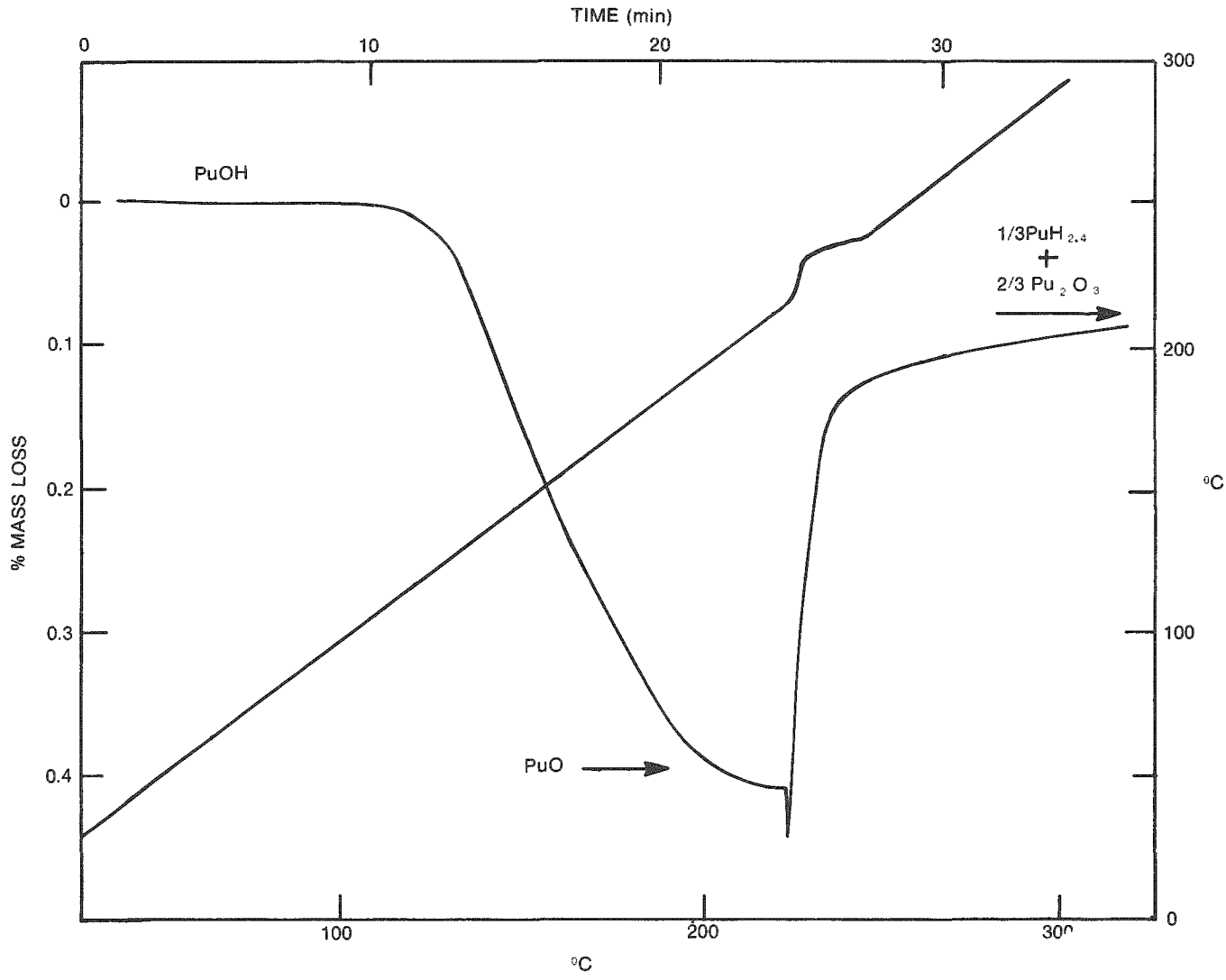


FIGURE 9. Thermogravimetric Results for Decomposition of PuOH Under 200 Torr $H_2$ Pressure at a Heating Rate of 7.7 °C·min$^{-1}$

and breaks at rational stoichiometric $H_2$ :Pu ratios cannot be explained in the absence of equilibrium. For example, the equilibrium process for the second equation in Table 5 is described in Equation 5.

$$7/8\ PuOH(s) + 1/4\ H_2O(\ell) \rightarrow 1/8\ Pu_7O_9H_3 + H^*\ (soln) \qquad (5)$$

The identity of the soluble hydrogen species, H*, is not known, but its concentration is fixed by the equilibrium process. Since the rate of formation of gaseous $H_2$ is proportional to the concentration of that species, the measured rate of hydrogen generation is constant until the PuOH phase is depleted. At that point, a lower H* concentration is established in the $Pu_7O_9H_3 + Pu_2O_3$ region and a new constant rate of hydrogen production is established. The PVT measurements simultaneously provide results about the kinetics and equilibria of the corrosion processes.

## Chemistry of the Pu+O+H System

Numerous reports have appeared on the dissolution of the lanthanide and actinide metals in aqueous

media. An insoluble residue is frequently formed during attempts to dissolve plutonium in dilute mineral acids or solutions of weak acids.[8] The residues are thought to be plutonium hydroxides or hydrated oxides.[9] Plutonium hydride also reacts with water to form a fine black powder.[8] A recent study indicates that the insoluble residues formed by lanthanide elements in weak acid solutions contain hydridic hydrogen.[10] These products are probably oxide hydrides similar to those observed in this study.

The chemistry of the Pu+O+H system is more complex than could ever be envisioned from earlier reports. A tentative phase diagram for the ternary system is presented in Figure 10. Three previously unknown plutonium oxide hydride phases (PuOH, $Pu_2O_2H$ and $Pu_7O_9H_3$) and four previously unreported plutonium oxide phases ($Pu_7O_{12}$, $Pu_9O_{16}$, $Pu_{10}O_{18}$, and $Pu_{12}O_{22}$) are shown. Equilibrium phase fields of the hydrolysis reactions are shown, although equilibrium involving the $H_2$ overpressure has not been attained in this study (see footnote to Table 4). Although the existence of plutonium monoxide has been described in earlier reports, those products are obtained only as surface layers and have been shown to be stabilized by carbon.[5] The characterization of the phases encountered

FIGURE 10. The Tentative Phase Diagram for the Pu+O+H System at 25 °C

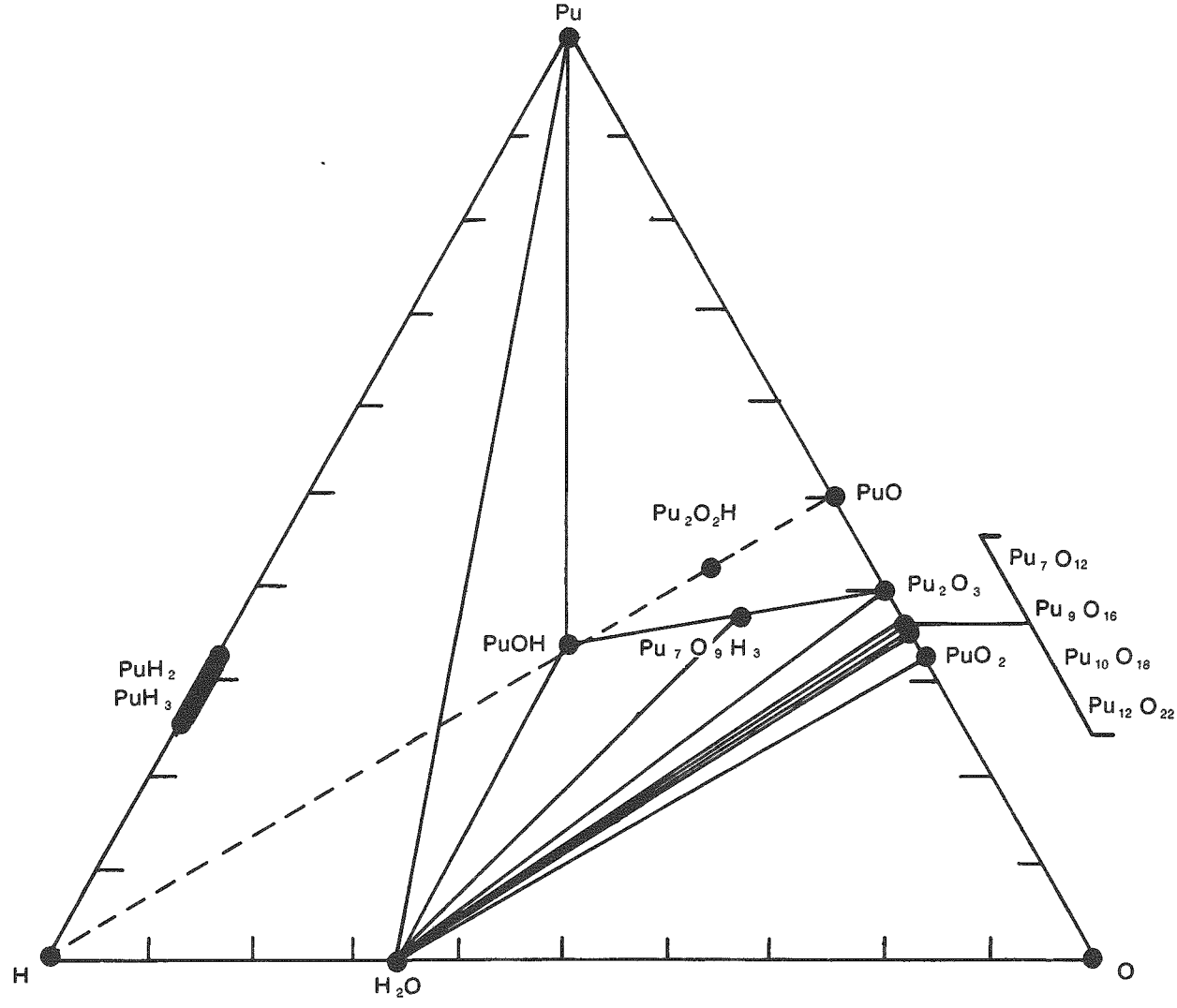

in this study is far from complete, but an interesting structural relationship and a structurally controlled sequence of reactions are suggested by Figure 10. $CaF_2$-type $PuH_2$ and the structurally related anion excess $PuH_{2+x}$ solid solution are well known. On the opposite side of the diagram, $CaF_2$-type $PuO_2$ and anion deficient $CaF_2$-related $Pu_2O_3$ are also well known. The existence of $CaF_2$-related PuOH has been established in this study. Although the hydrolysis of $PuH_2$ remains to be studied, earlier observations suggest that the solid product is PuOH.[8] This proposed process is the first step in a sequence of reactions in which hydrogen on a lattice site in a $CaF_2$-type (or $CaF_2$-related) structure is successively replaced by oxygen. The PuOH phase is a structural analog of $PuO_2$, but contains trivalent plutonium, oxide and hydride. During the formation of $Pu_7O_9H_3$ from PuOH, 4/7 of the $H^-$ions in the monoxide monohydride are replaced by half that number of $O^{2-}$ions to form $Pu_7O_9H_3$ and $H_2$ gas. The product phase contains Pu(III) and is probably a structural analog of the $CaF_2$-related defect oxides $UY_6O_{12}$ and $Pr_7O_{12}$. (See Reference 11.) Continued hydrolysis of $Pu_7O_9H_3$ to $Pu_2O_3$ results in complete replacement of $H^-$ions and formation of $Pu_2O_3$. The reaction sequence continues to generate $H_2$, but its formation is based on the oxidation of Pu(III) to Pu(IV) and then to an oxidation state higher than Pu(IV). The intermediate oxides between $Pu_2O_3$ and $PuO_2$ contain different ratios of Pu(III) and Pu(IV) and correspond exactly with the $CaF_2$-related defect oxides of praseodymium.[11] The production of gas at apparent $H_2$:Pu ratios greater than 2.00 is difficult to explain. Since gas analysis shows that high concentrations of $O_2$ are present in the product, this behavior is attributed to radiolytic decomposition of water. At $H_2$:Pu<2.00, oxygen species apparently react with the solid and $O_2$ is not formed.

A sequence of reactions based on thermal decomposition is also indicated by the dashed line in Figure 10. On heating, PuOH disproportionates to form $H_2$ and the transient phase $Pu_2O_2H$, which is possibly a structural analog of $CaF_2$-related $Pu_2O_3$. Such $M_2O_2X$ derivative phases are well known for the lanthanides with X as dicarbide, sulfide, selenide or telluride. Thermal decomposition of $Pu_2O_2H$ yields $H_2$ and PuO. Although structural data are not available for the monoxide, the phase has interesting structural possibilities, and speculation involves a topotactic relationship to possible structures of PuOH and $Pu_2O_2H$. It is a reasonable possibility that the anions in PuOH are not randomly positioned on the tetrahedral sites, but are ordered with the oxygens and hydrogens on interlocking ZnS-type sublattices. Retention of oxide order on heating would lead to a ZnS-type monoxide; however, one might expect the phase to have a NaCl-type structure. The system provides an opportunity for an interesting study. At sufficiently high temperatures, the metastable monoxide disproportionates into $Pu_2O_3$ and Pu.

Another interesting aspect of PuOH decomposition is the close correspondence of its decomposition behavior with that of the hysteresis loop observed in the plutonium hydride equilibrium system.[7]

A particularly important result of this study is its impact on the phase diagram of plutonium + oxygen. The stability of the intermediate oxides belonging to the homologous series $Pu_nO_{2n-2}$ with n = 7, 9, 10, and 12 has been established. In the region $Pu_2O_3$ to $PuO_2$, the Pu + O diagram is apparently very similar to that of Pu + O.[11] It is interesting that plutonium hydroxides are not encountered in the course of hydrolysis. This observation implies that the hydroxides are unstable relative to the oxides and water.

Hydrolysis of plutonium and of the series of oxide hydrides and oxides inherently behaves like a hydrogen titrimeter and provide unique insight into the chemistry of the Pu+O+H system. The technique should be useful for parallel studies of lanthanides and other actinides and may well provide a novel low temperature method for preparing their monoxides.

## REFERENCES

1. A. E. Hodges III, J. J. Reynolds, and J. M. Haschke, "Corrosion of Delta Plutonium in Rocky Flats Tap Water," USDOE Report RFP-2891, Rocky Flats Plant, Golden, Colorado, 80401. September 1979

2. A. E. Hodges III and J. M. Haschke, "Corrosion of Delta Plutonium by Synthetic Sea Water," USDOE Report RFP-2919, Rocky Flats Plant, Golden, Colorado, 80401. October 1979

3. E. T. Lance-Gómez and J. H. Haschke, "Phase Equilibria of the Oxide-Hydroxide + Halide Systems of Sm, Eu, and Gd. The Crystal Structure of $Gd_3O(OH)_5Br_2$," Journal of Solid State Chemistry, Vol 35, p 357. 1980

4. H. Nowotney and K. Seifert, "Crystal Structures and Densities in Plutonium: Physico-Chemical Properties of its Compounds and Alloys," Atomic Energy Review, International Atomic Energy Agency, Vienna, p 73. 1966

5. D. T. Larson and J. M. Haschke, "XPS-AES Characterization of Plutonium Oxides and Oxide Carbide. The Existence of Plutonium Monoxide," Inorganic Chemistry, Vol 20, p 1945. 1981

6. J. M. Haschke and J. L. Stakebake, "Decomposition Kinetics of Plutonium Hydride," USDOE Report RFP-2878, Rocky Flats Plant, Golden, Colorado 80401. January 1980

7. J. M. Haschke, "Thermodynamic Properties of the Cubic Plutonium Hydride Solid Solution," USDOE Report RFP-3099, Rocky Flats Plant, Golden, Colorado, 80401. 1981

8. J. M. Cleveland, "The Chemistry of Plutonium," Gordon and Breach Science Publishers, New York. 1970

9. W. N. Miner, A. S. Coffinberry, F. W. Schonfeld, J. T. Waber, R. N. R. Mulford, and R. E. Tate, "Plutonium in Rare Metals Handbook," C. A. Hampel, Ed., Reinhold Publishing Corp., London, Chapter 18. 1961

10. G. L. Silver, "New Hydridic Rare Earth Compounds in The Rare Earths in Modern Science and Technology," G. J. McCarthy, J. J. Rhyne, and H. B. Silber, Eds., Vol 2, Plenum Press, New York, p 605. 1980

11. L. Eyring, "The Binary Rare Earth Oxides in Handbook on the Physics and Chemistry of Rare Earths," K. A. Gschneidner and L. Eyring, Eds., North Holland Publishing Co., Amsterdam, Vol 3, Chapter 27. 1979